

Integration of solar thermal systems in existing district heating systems

Carlo Winterscheid¹, Jan-Olof Dalenbäck¹ and Stefan Holler²

¹ Chalmers University of Technology, Gothenburg (Sweden)

² HAWK University of Applied Science and Arts, Göttingen (Germany)

Abstract

The integration of large solar heating systems in district heating (DH) networks with large combined heat and power (CHP) plants is rarely considered. This is often due to low costs for heat but also due to subsidies for the electricity by CHP plants. Possible changes in subsidies and requirements in the reduction of fossil fuel based CO₂ emissions raise an awareness of improving the operational flexibility of fossil fuelled CHP plants. This paper provides a rather simple but detailed methodology of including large solar heating systems in an existing district heating system, where heat is supplied by a large CHP plant. It uses hourly data of load and temperature patterns as well as radiation data and collector efficiency data to determine collector field size and storage size. The possibility of largely independent operation of sub-networks is analysed, which allows different system temperatures. A feasibility study indicates specific heat generating costs for different collector types. It is demonstrated that a sub-network can operate without a back-up boiler and that both network parts benefit from the interaction.

Keywords: *district heating, solar district heating, solar thermal systems*

1. Introduction

The integration of solar thermal systems in DH systems is a more and more common practice in some countries; however, few studies have been performed on methodologies and benefits of integrating solar thermal systems in DH systems that are mainly supplied by large scale CHP plants with low heat generation costs.

The general idea behind including solar collector fields in DH networks is to lower or even completely supply the low heat demand of a DH network during the summer months. Since the 1980s Denmark and Sweden have built many solar heating plants (Fisch et al. 1998). In some of these cases a seasonal storage is used to provide a solar share even above 50 % of the total system demand. The high taxation of primary energy sources supported the ambitions in Denmark that lead to seasonal storages which are only feasible in a very large scale (Meißner et al. 2012). In comparison to the Danish and Swedish developments solar DH systems in Germany started to be built later, at the beginning of the 1990s.

The large DH systems in Germany are generally supplied by large CHP plants. These plants are often operating as base load power producers and can supply heat and electricity at a cost-efficient level during summer and winter due to funding through the CHP production law (KWKG) (Berberich et al. 2015). In addition to the availability of low-cost heat, high and very high system temperatures in the DH systems also prevented solar heat generating systems (Urbanek et al. 2015). In the case of the DH system Chemnitz, only a large change in the system structure in one district made a change feasible. Possibilities of including solar collector systems in existing DH networks that are not about to change radically and are using large scale CHP plants as a main heat source were rarely analysed. Despite of the higher specific generation costs a solar collector field can also bring several advantages to systems of the mentioned kind.

This paper presents aspects where a solar collector field can be beneficial for a DH system based on a large scale CHP plant and how such a collector field can be included. The work was carried out by evaluating the load pattern of a part of an existing DH system in Germany. In the given case the system analyse was based on the following conditions:

- A fixed supply temperature in a connected sub-network that is not needed in the whole system
- A long connection pipeline between the main network plant and the connected sub-network
- A reduction of the primary energy factor (PEF)
- A reduction in CO₂ emissions

Taking into account the interests of the network owner different methodologies of including a solar collector field were developed. In the given case a solution without a local backup boiler is preferred; instead a daily reheat of a storage from the large CHP plant was suggested.

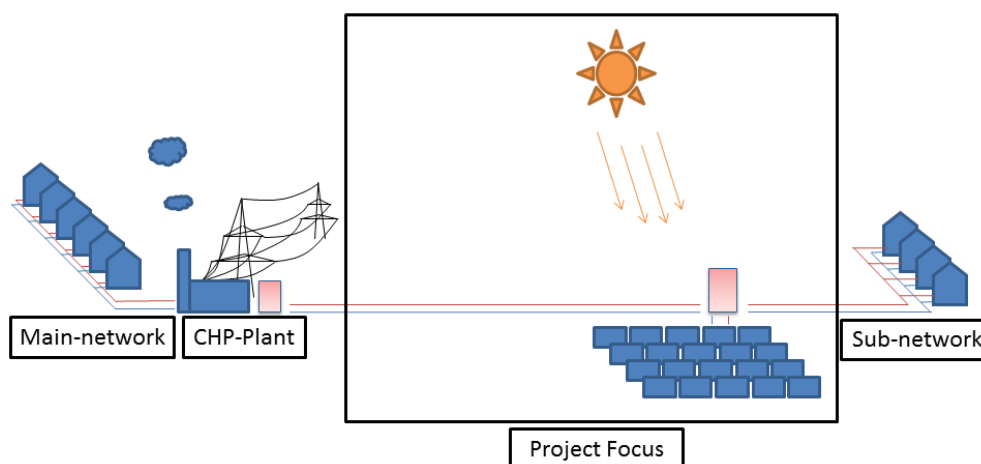


Figure 1. Project focus: The solar thermal field and the thermal storage are located between main-network and sub-network

2. Methodology

The calculations for this project have been performed in MATLAB and are based on four years of measurements of heat consumption, volume flow and flow temperatures. Values in 15 min time steps for the solar radiation of an average day of each month were imported from PVGIS (European Commission) for the specific location. Additional weather evaluation has been performed using outdoor temperature data from 1974 to 2014 from Germany's National Meteorological Service (DWD) (Deutscher Wetterdienst).

Figure 2 below visualizes the methodology in a flow-chart starting with the input over a decision in solar share, resulting in collector areas, storage sizes and finally an energy flow overview and a storage operation visualization.

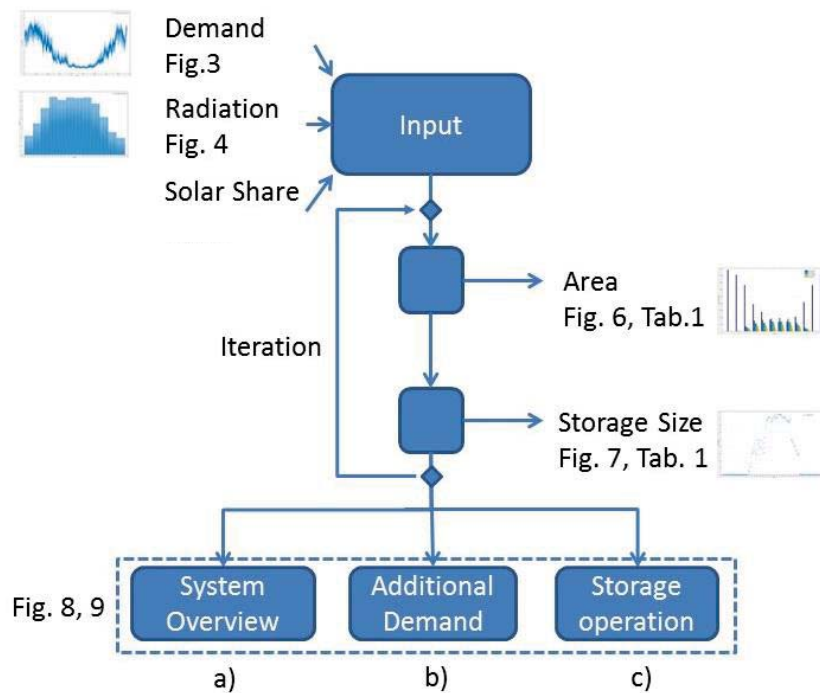


Figure 2. Methodology for the integration of solar heat into existing DH systems

Figure 3 shows the average heat load $Q_{dem,av}$ of the given consumer, the sub-network of the years 2013-2015. The following figure 4 shows the solar radiation during a year on a surface tilted south with an angle of 35° .

Based on the smoothed outdoor temperature line of the average outdoor temperature from 1974 to 2014 given by DWD (Deutscher Wetterdienst) and a graph displaying the required supply temperature to the sub-network, the time span from hour 3241 to hour 6337 of a year was calculated when the supply temperature is at its allowed minimum (Figure 5). In this time span the DH main-network could further decrease the supply temperature, if it could operate independently of the sub-network. The focus of this project was how the sub-network can be supplied by a solar heating system during this period.

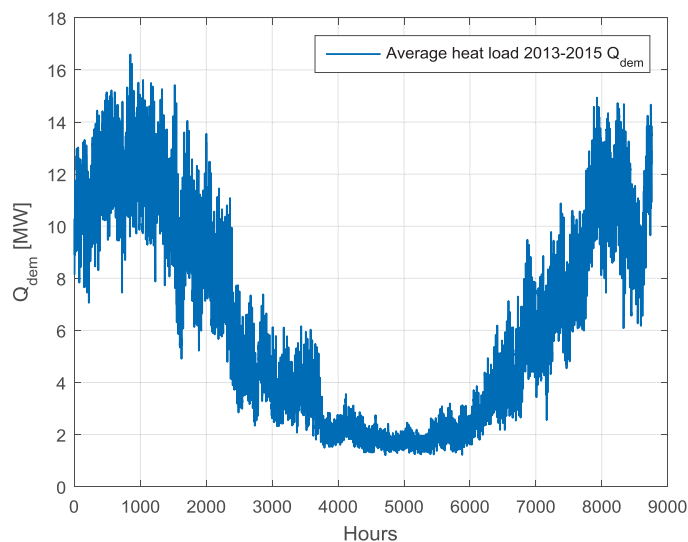


Figure 3. Example of annual the heat load curve in a sub-network

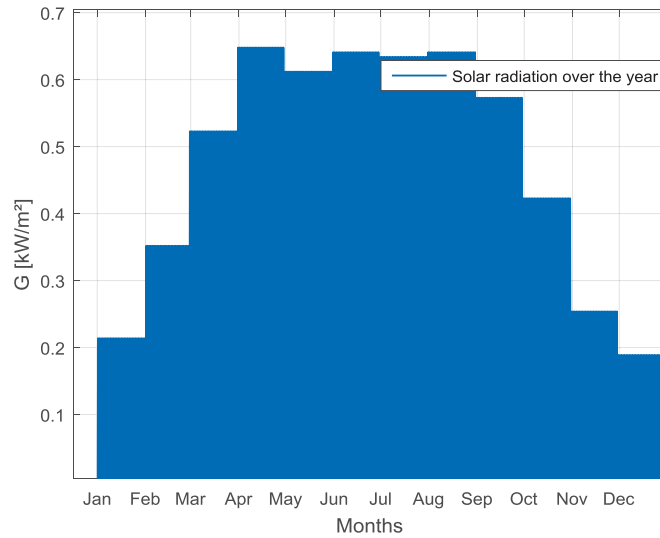


Figure 4. Example of maximum solar radiation on an average day on a south oriented 35° tilted surface in southern Germany

The efficiency of solar collectors η_c was calculated according to the European Standard EN 12975 (Kovacs 2012) as follows:

$$\eta_c(t) = \eta_0 - a_1 \frac{(T_m(t) - T_a(t))}{G(t)} - a_2 \frac{(T_m(t) - T_a(t))^2}{G(t)} \quad (\text{Eq. 1})$$

$$T_m(t) = \frac{(T_{out}(t) + T_{in}(t))}{2} \quad (\text{Eq. 2})$$

η_0 Collector zero-loss efficiency (-)

a_1 First degree coefficients of the collector heat losses (W/Km²)

a_2 Second degree coefficients of the collector heat losses (W/Km²)

G Global radiation (W/m²)

T_m Hourly medium temperature (K)

T_a Hourly ambient temperature (°C)

T_{out} Hourly collector outlet temperature (°C)

T_{in} Hourly collector inlet temperature (°C)

Accordingly, the net solar gain $Q_{sol}(t)$ is:

$$Q_{sol}(t) = \eta_c(t) * G(t) \quad (\text{Eq. 3})$$

As the average global irradiance ins given in 15 minute steps the resolution was reduced to hourly steps in order to use the actual DH return temperature as collector inlet temperature T_{in} and the DH supply temperature as the collector outlet temperature T_{out} if it was above 80 °C, otherwise T_{out} was set to 80°C. The ambient temperature T_a was taken from PVGIS as well. The collector dependent values η_0 , a_1 and a_2 were taken from collector datasheets of a Arcon HT-HEATboost 35/10- flat plate collector (FPC) and a RitterXL XL 19/49P evacuated tube collector (ETC).

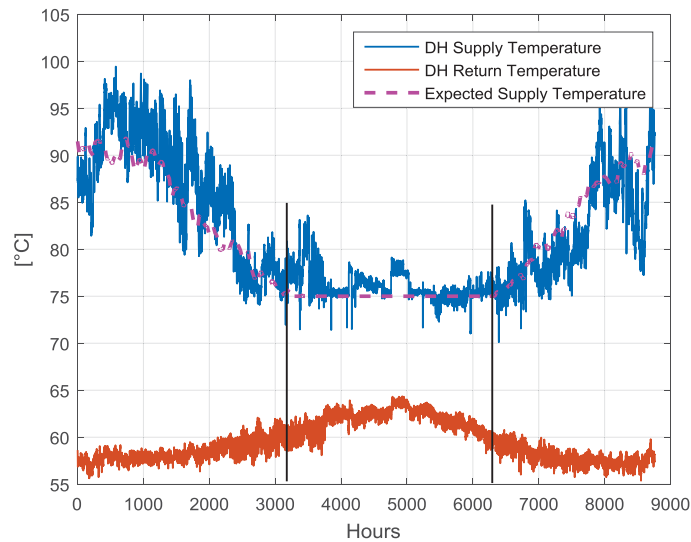


Figure 5. Average supply and return temperature and expected supply temperature of the sub-network

2.1 Area selection

Field sizes were calculated depending on different annual solar shares of 5 %, 10 %, 15 % and 20 % of the total annual heat consumption. Additionally, one approach aims to supply the heat consumption of July completely, which corresponds to 14 % solar share, because this is the month with the lowest consumption throughout the year. The following calculation steps are used to receive the actual collector aperture area in m²:

$$Rel(t) = \frac{Q_{dem,m}(t)}{Q_{dem,tot}} \quad (\text{Eq. 4})$$

$$Q_{sol,m}(t) = Q_{sel} * Rel(t) \quad (\text{Eq. 5})$$

$$A = \max \left(\frac{Q_{sol,m}(t)}{q_{sol,m}(t)} \right) \quad (\text{Eq. 6})$$

Rel Relative monthly energy demand (-)

$Q_{dem,m}$ Monthly energy demand by the sub-network (kWh)

$Q_{dem,tot}$ Annual energy demand by the sub-network (kWh)

$Q_{sol,m}$ Monthly energy to be supplied by solar (kWh)

Q_{sel} Annual energy chosen to be supplied by solar (kWh)

$q_{sol,m}$ Specific net solar gain per month (kWh/m²)

A Aperture area needed (m²)

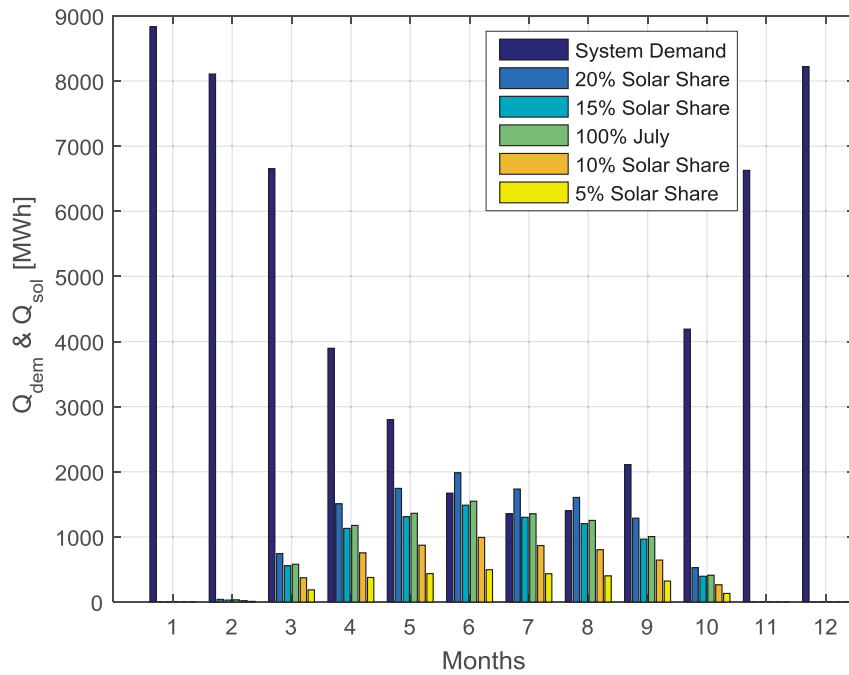


Figure 6. Net solar gain compared to demand for different solar share variations

Figure 6 shows an overview of the different solar shares compared to the monthly energy demand. At an annual solar share of 14 % the solar heat energy fully covers the heat demand in the month of lowest demand (July). A higher annual solar share provides a surplus of solar heat during the summer that cannot be used.

Table 1 shows an overview of the calculated variations with the collector area, the relative storage dimension and the achieved CO₂ savings.

Table 1. Calculation results for different annual solar share

Solar share	Collector area (m ²)	Specific storage volume (l/m ²)	Storage volume (m ³)	CO ₂ savings (t/a)
5 %	6507	7.3	50	480
10 %	13029	30.3	403	961
14 %	18319	39.5	728	1348
15 %	19536	40.5	802	1424
20 %	26044	46.2	1220	1725

2.2 Storage dimensioning

For this project it was required to store only the surplus solar heat that can be received within a single day and dimension the storage size accordingly. Figure 7 shows the solar surplus of each day that can be received when having an average load and a solar collector field size corresponding to the July demand (annual solar share of 14 %).

The conversion from MWh storage capacity to m³ water in storage capacity was performed according to the following formula:

$$V = \frac{Q_{st}}{\rho * c * (T_{max} - T_{min})} \quad (\text{Eq. 7})$$

V Storage volume (m³)

Q_{st} Storage energy capacity (MWh)

ρ Density of water (kg/m³)

c Heat capacity of water (Wh/(kg*K))

T_{max} Maximum storage temperature (°C)

T_{min} Minimum storage temperature (°C)

T_{min} is the maximum return temperature measured, 63 °C and T_{max} is the maximum allowed temperature in the storage 95 °C.

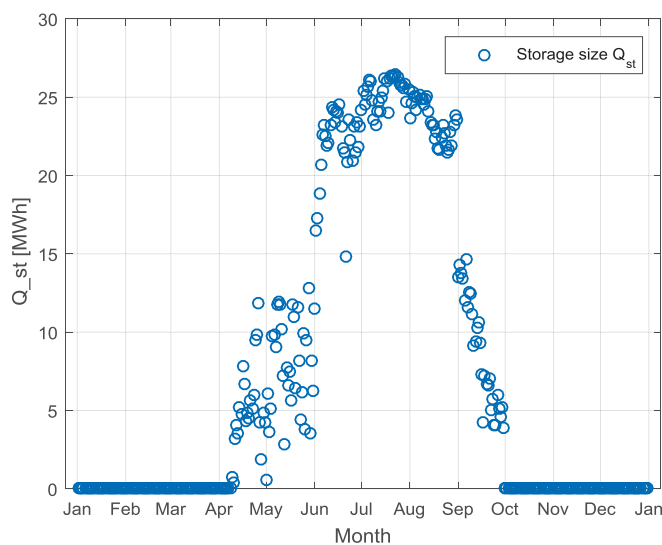


Figure 7. Needed storage capacity to store the solar surplus energy

2.3 Storage operation

To enable the sub-network to operate as independently as possible without having a backup boiler it is considered that the storage is reheated once per day. In this scenario the recharge from the main-network is set to be done every evening at 21.00 h with a supply temperature of 80 °C. This means that during summer time 3 different temperature zones will develop in the storage; one with the DH return temperature, one with 80 °C from the CHP plant and one with a maximum of 95 °C from the collector field.

2.4 Iteration

At this point an iteration is needed because the collector efficiency calculation depends on the DH supply and return temperatures that influence the collector inlet and outlet temperatures. To utilize the thermal storage to its maximum the storage temperature was set to a maximum of 95 °C. For the days that the storage is charged to its maximum the collector outlet temperature needs to be at least 95 °C. With the adjusted temperatures and thereby changed efficiencies the area and storage calculation was repeated.

3. Results

The first thing to realize throughout the calculation was that the needed storage size to store a solar surplus was below 50 l/m² collector area. A relatively small dimensioned storage is also recommended by Meißner et al.. Meißner et al. also points out that a solar storage is normally not used for the largest part of the year. This statement is also visually confirmed in Figure 7.

Figure 8a shows the supply and demand curves for the summer season if a recharge every evening is done for a solar collector area of 18,319 m² which corresponds to 14 % solar share. Figure 8 b) shows the additional demand of the system, meaning the heat power that is needed at some hours to cover the demand of the sub-network if the storage is empty and not enough direct solar energy is available. Equation (8) below shows the relation between the different heat power terms:

$$\dot{Q}_{dem} = \dot{Q}_{sol,dir} + \dot{Q}_{dis} + \dot{Q}_{add} \quad (\text{Eq. 8})$$

\dot{Q}_{dem} Heat load of the sub-network (MW)

$\dot{Q}_{sol,dir}$ Directly used solar heat rate (MW)

$\dot{Q}_{sol,stor}$ Stored solar heat rate (MW)

\dot{Q}_{dis} Storage heat discharge rate (MW)

\dot{Q}_{add} Additional heat supply rate (MW)

Q_{re} Daily storage heat energy recharge (MWh)

Q_{ch} Level of storage charge (MWh)

Figure 8c and 9c display the storage charge and the energy the storage is charged with during the reheating process. In Figure 9a it can also be seen that when the storage is recharged, \dot{Q}_{dem} of the sub-network at that moment is covered by the main-network, too.

While Figure 8 presents the complete summer season of a system with 14 % solar share, Figure 9 shows the supply and demand for the same system but this time only for 4 days. In Figure 9c, the excerpt of Figure 8c, it becomes visible that a regular evening recharge enables a projectable operation of main- and subnetwork. When analysing the red state of charge line in Figure 8c one can see that a daily recharge is not even needed every day.

The optimal system choice is therefore an offset between a system that needs as little additional energy during the summer season as possible, with the aim to let the main-network operate as independent as possible and a system that has a collector area as little as possible to reduce the system costs as well as to reduce the losses during the summer due to storage limitations.

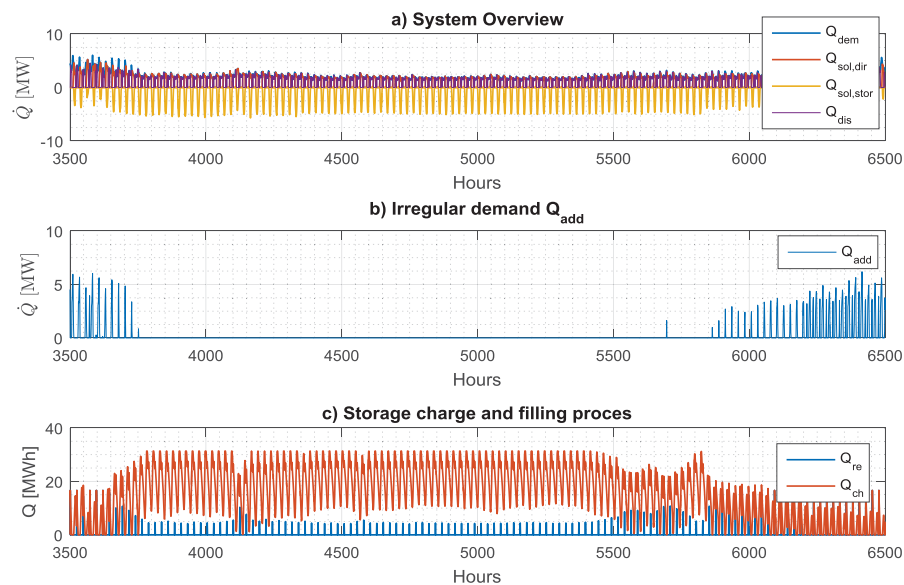


Figure 8. Supply and demand curves (a), additional heat power demand (b) and storage charging (c) during the summer season with 14 % solar share

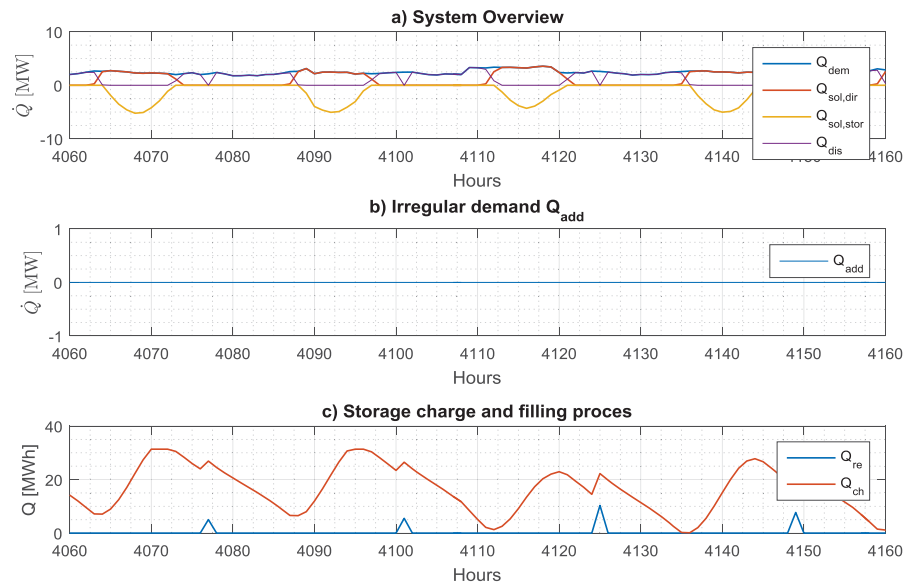


Figure 9. Zoomed in 4 days of supply and demand for the scenario with 14 % annual solar share

\dot{Q}_{dem}	Heat load of the sub-network	(MW)
$\dot{Q}_{sol,dir}$	Directly used solar heat rate	(MW)
$\dot{Q}_{sol,stor}$	Stored solar heat rate	(MW)
\dot{Q}_{dis}	Storage heat discharge rate	(MW)
\dot{Q}_{add}	Additional heat supply rate	(MW)
Q_{re}	Daily storage heat energy recharge	(MWh)
Q_{ch}	Level of storage charge	(MWh)

Figure 8 shows that a system of the given specification can supply the sub-network's demand during the summer season to a large extent independently of the main-network if an overnight charging of the storage to 80 °C is given. An increase from 14 % solar share to 20 % solar share will reduce the need for additional energy supply from the main network during the summer season but will also increase the losses of solar energy as the storage is not emptied for the largest part of the summer season. Furthermore, the difference in the collector area between 14 % and 20 % solar share is 7725 m² and will also have a large economic impact.

Additionally, a decrease in CO₂ emissions, as visible in Table 1, is possible by up to 1725 t CO₂ per year in the case of 20 %.

4. Feasibility study

The economic analysis of the calculated system is based on the main components as collectors, storage and the cost of land. Additional costs as control technology, system technology, construction works, planning and costs for system integration were added in percentage on the sum of the costs of the main components according to Schmidt & Deschaintre. The discounting of the investment costs is performed over 25 years and an interest rate of 4 % is applied. The collector costs used are 200 €/m² (Trier 2015) for flat plate collectors and 340 €/m² (AGFW 2013) for evacuated tube collectors. Cost of land were in this calculation set to 9 €/m² and the specific costs for the thermal storage were set to 140 €/m³ (Maripuu & Dalenbäck 2011).

Additional subsidies based on German legislation were taken into account for this example system. According to (Pauschinger) 40 % of the collector costs and 30 % of the storage cost can be subsidized in Germany.

The following figure 10 shows the specific heat generating costs depending on the collector costs. The turn in both collector type lines at about 15 % solar share can be explained with the maximal capacity of the short-term thermal storage. If the collector area is too large the solar gains per day exceed the demand of the DH network per day.

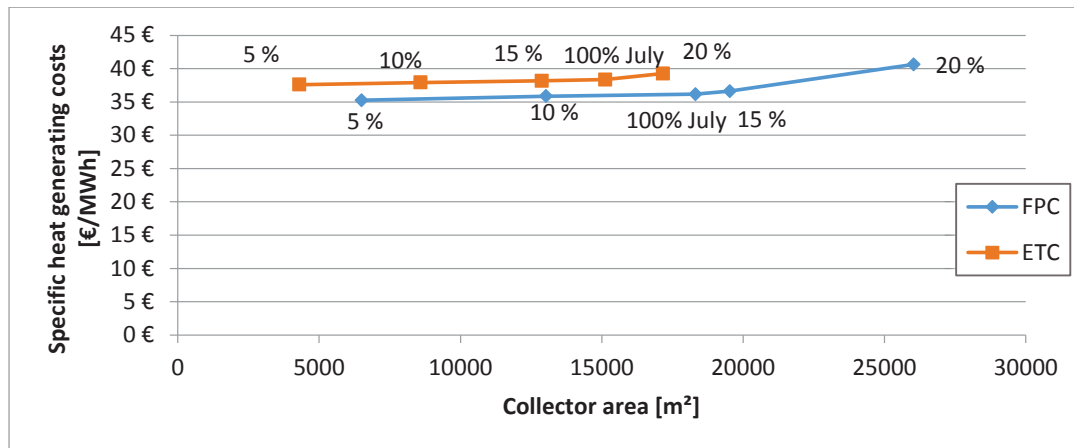


Figure 10. Specific heat generating costs dependent on the collector area for both collector types.

Figure 11 shows that the annual cost per amount of CO₂ reduced develop rather linear for both collector types until about 15 % when the issue of the storage limitation and too low network demand change the balance.

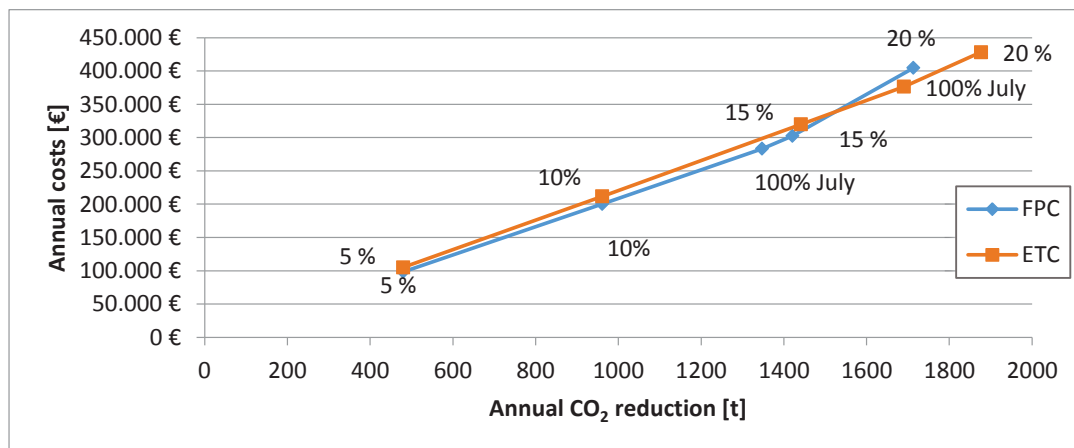


Figure 11. Annual system costs depending on the annual achievable CO₂ emission reduction

5. Discussion

The comparison of the presented results against results of a freeware calculation tool (SDH Online-Calculator (Solites & AGFW)) with similar input data shows a generally good validity of the method. However, due to different methodological approaches the results cannot be compared to each other directly.

Firstly, the irradiation on the collector field was about 16 % higher in this project. This is due to a different location that was chosen but most of all due to the different meteorological data source of both calculations.

Secondly, it has to be mentioned that losses in the piping system and the storage of about 5 to 10 % have to be added.

Thirdly, results in the CO₂ savings differ in this project compared to the SDH-Online tool as the CO₂-emission factor of 172 g/kWh for the given example DH system was used.

The reader also has to be aware that small variations on the specific collector price [€/m²] have huge influence on the overall costs as the collector costs account for 70% of the whole system costs. The collector prices are changing depending on the system size, the location and are also expected to change over time.

6. Conclusion

The integration of solar heat into existing DH systems brings benefits to a fossil CHP plant based system such as CO₂ reduction, primary energy factor improvement and a larger operational flexibility. The possibility to supply a sub-network for certain periods of the year mainly by solar heat, allows an increasing efficiency of the CHP plant in the main network for the time that the temperatures can be lowered.

Furthermore, a solar thermal system enables the whole DH network to react better on future changes in the German electricity price market when it may be economically beneficial to decrease the energy production of the plant from an electricity production point of view.

The study shows that the accuracy of dimensioning a solar district heating system highly depends on the quality of the input data used. Calculations on the basis of annual data provide a rough idea on the necessary collector area and storage volume for a given heat demand. However, an exact dimensioning can only be done by using hourly-data of solar radiation and heat load for a whole year period.

The methodology for the integration of solar heat into DH systems that is presented in this paper leads to more detailed results and avoids over-dimensioning of solar fields and storage volume.

The example calculation shows that a solar thermal DH sub-network with a thermal storage and an annual solar share of 14 % can be realized without auxiliary gas or biomass boiler, if the main-network can adapt to a lack of heat power in the sub-network. The option of a regular recharge of the storage makes the operation of the centralized CHP plant more predictable. During the summer months the solar heat gains cover the total heat demand of the sub-network for long periods, whereas in other times of the year the main-network provides the additional heat. A short-term storage with a specific volume below 40 l/m² is sufficient under the here give load pattern.

7. Outlook

The results of the presented calculations can be improved by optimizing the storage recharging time and level as well as by adding the piping system as a temporary storage. In the example of a DN300 pipe without extractions an additional specific volume of 78 m³/km can be taken into account to store water at 80 °C for a short time once a day. In this case a focus will also have to be put on the losses over the pipeline.

Finally, the methodology needs to be applied on an operating SDH system.

8. References

- AGFW, 2013. Transformationsstrategien Fernwärme, Frankfurt am Main.
- Berberich, M. et al., 2015. SOLAR-KWK Entwicklung multifunktionaler Systeme zur solar unterstützten Kraft-Wärme-Kopplung – solare Fernwärme und saisonale Wärmespeicher für die Energiewende, Stuttgart.
- Deutscher Wetterdienst, DWD Deutscher Wetterdienst. Available at: <http://www.dwd.de/DE/leistungen/klimadatendeutschland/klimadatendeutschland.html> [Accessed May 10, 2016].
- European Commission, PV GIS. Available at: <http://re.jrc.ec.europa.eu/pvgis/apps4/pvest.php#> [Accessed May 10, 2016].
- Fisch, M., Guigas, M. & Dalenbäck, J.-O., 1998. A review of large-scale solar heating systems in Europe. *Solar Energy*, 63(6), pp.355–366. Available at: <http://www.sciencedirect.com/science/article/pii/S0038092X98001030>.
- Kovacs, P., 2012. A guide to the standard EN 12975, Borås.
- Maripuu, M. & Dalenbäck, J.-O., 2011. SUNSTORE 4 WP5 - European level concept study Feasibility / simulation studies, Göteborg.
- Meißner, R. et al., 2012. Sinn und Unsinn von Solarspeichern. *FEE Heizungsjournal - Special*, pp.1–6.
- Pauschinger, T., 2015. Solnet BW Solare Wärmenetze für Baden-Württemberg Grundlagen | Potenziale | Strategien, Stuttgart.
- Schmidt, T. & Deschaintre, L., 2013. SDH online-rechner. Available at: <http://www.sdh-online.solites.de/Content/media/SDH-Online-Rechner.PDF>. [Accessed May 10, 2016]

Solites & AGFW, SDH Online-Calculator. Available at: www.sdh-online.solites.de [Accessed May 10, 2016].

Trier, D., 2015. Solare Fernwärme in Dänemark - Entwicklungen und Trends. *Erneuerbare Energie*, 3. Available at: www.aee.at/aee/index.php?option=com_content&view=article&id=870&Itemid=113.

Urbaneck, T. et al., 2015. Solar District Heating in East Germany – Transformation in a Cogeneration Dominated City. *Energy Procedia*, 70, pp.587–594. Available at: <http://www.sciencedirect.com/science/article/pii/S1876610215002866>.